

# Dissociation of Relativistic Projectiles with the Continuum-Discretized Coupled-Channels Method

Kazuyuki OGATA<sup>1</sup> and Carlos A. BERTULANI<sup>2</sup>

<sup>1</sup>*Department of Physics, Kyushu University, Fukuoka 812-8581, Japan*

<sup>2</sup>*Department of Physics, Texas A&M University, Commerce, TX 75429, USA*

Relativistic effects in the breakup of weakly-bound nuclei at intermediate energies are studied by means of the continuum-discretized coupled-channels method with eikonal approximation. Nuclear coupling potentials with Lorentz contraction are newly included and those effects on breakup cross sections are investigated. We show that relativistic corrections lead to larger breakup cross sections. Coupled-channel effects on the breakup cross sections are also discussed.

Reactions with radioactive nuclear beams are a major research area in nuclear physics. The dissociation of weakly bound nuclei, or halo nuclei, is dominated by the Coulomb interaction, although the nuclear interaction with the target cannot be neglected in most cases.<sup>1)</sup> The final state interaction of the fragments with the target, and between the themselves, leads to important continuum-continuum and continuum-bound-state couplings which appreciably modify the reaction dynamics. Higher-order couplings are more relevant in the dissociation of halo nuclei due to their low binding.<sup>2),3)</sup>

The continuum-discretized coupled-channels method (CDCC)<sup>4)</sup> is one of the most accurate models to describe the breakup of halo nuclei taking account of higher-order couplings explicitly. The eikonal CDCC method (E-CDCC),<sup>2),3)</sup> which was developed by the Kyushu group, is a derivation of CDCC that enables one to efficiently treat the nuclear and Coulomb breakup reactions at  $E_{lab} \geq 50$  MeV/nucleon. An essential prescription described in Refs. 2),3) is the construction of hybrid (quantum and eikonal) scattering amplitudes, with which one can make quantum-mechanical (QM) corrections to the pure eikonal wavefunctions with a minimum task. These corrections are, however, expected to become less important as the incident energy increases.

The eikonal CDCC equations are Lorentz covariant in the high energy limit as shown later. However, this is only true if the Coulomb and nuclear potentials used in the calculations are correspondingly Lorentz covariant. This has not been explored, except for the calculation presented in Ref. 5). In fact, most rare isotope facilities use projectile dissociation at 100–250 MeV/nucleon. At these energies, relativistic contraction of fields and retardation effects<sup>6)–9)</sup> are of the order of 10–30 %. Relativistic effects enter in the dynamics of coupled-channels equations in a nonlinear, often unpredictable way, which can lead to a magnification, or reduction, of the corrections. In the present work, we confirm the relevance of the relativistic effects mentioned above, henceforth called dynamical relativistic effects, on the breakup cross sections of <sup>8</sup>B and <sup>11</sup>Be nuclei by <sup>208</sup>Pb target at 100 and 250 MeV/nucleon. We make use of E-CDCC incorporating relativistic Coulomb and nuclear coupling potentials. The

role of the latter, a novel effect included in this work, is investigated. We also see how the channel-coupling affects the breakup cross section with and without dynamical relativistic effects.

The multipole-expansion of the relativistic Coulomb potential between the target nucleus (T) with the atomic number  $Z_T$  and the projectile (P), consisting of C and v clusters, are given in Ref. 5):

$$V_{E1\mu} = \sqrt{\frac{2\pi}{3}} \xi Y_{1\mu}(\hat{\xi}) \frac{\gamma Z_T e e_{E1}}{(b^2 + \gamma^2 z^2)^{3/2}} \begin{cases} \mp b & (\text{if } \mu = \pm 1) \\ \sqrt{2}z & (\text{if } \mu = 0) \end{cases} \quad (1)$$

for the E1 (electric dipole) field and

$$V_{E2\mu} = \sqrt{\frac{3\pi}{10}} \xi^2 Y_{2\mu}(\hat{\xi}) \frac{\gamma Z_T e e_{E2}}{(b^2 + \gamma^2 z^2)^{5/2}} \times \begin{cases} b^2 & (\text{if } \mu = \pm 2) \\ \mp(\gamma^2 + 1)bz & (\text{if } \mu = \pm 1) \\ \sqrt{2/3}(2\gamma^2 z^2 - b^2) & (\text{if } \mu = 0) \end{cases} \quad (2)$$

for the E2 (electric quadrupole) field. In Eqs. (1)–(2),  $e_{E\lambda} = [Z_v(A_C/A_P)^\lambda + Z_C(-A_v/A_P)^\lambda]e$  are effective charges for  $\lambda = 1$  and 2 multipolarities for the breakup of  $P \rightarrow C + v$ . The intrinsic coordinate of v with respect to C is denoted by  $\xi$  and  $b$  is the impact parameter (or transverse coordinate) in the collision of P and T, which is defined by  $b = \sqrt{x^2 + y^2}$  with  $\mathbf{R} = (x, y, z)$ , the relative coordinate of P from T in the Cartesian representation. The Lorentz contraction factor is denoted by  $\gamma = (1 - v^2/c^2)^{-1/2}$ , where  $v$  is the velocity of P. Note that these relations are obtained with so-called far-field approximation,<sup>10)</sup> i.e.  $R$  is assumed to be always larger than  $\xi$ . The Coulomb coupling potentials in E-CDCC are obtained with Eqs. (1)–(2) as shown below.

As for the relativistic nuclear potentials, we follow the conjecture of Feshbach and Zabek,<sup>11)</sup> in which Lorentz contraction was introduced in a nuclear potential inspired on the folding model. In the present work, we further make zero-range approximation to the folding model. Accordingly, we replace the non-relativistic optical potential  $U(\mathbf{b}, z)$  between T and each constituent of P by  $\gamma U(\mathbf{b}, \gamma z)$ . Even though this is a quite rough prescription to include the dynamical relativistic corrections on the nuclear potential, we can check effects of the correction on breakup cross sections at least semi-quantitatively.

The E-CDCC equations for the three-body reaction under consideration are given by:<sup>2),3)</sup>

$$\frac{i\hbar^2}{E_c} K_c^{(b)}(z) \frac{d}{dz} \psi_c^{(b)}(z) = \sum_{c'} \mathfrak{F}_{cc'}^{(b)}(z) \mathcal{R}_{cc'}^{(b)}(z) \psi_{c'}^{(b)}(z) e^{i(K_{c'} - K_c)z}, \quad (3)$$

where  $c$  denotes the channel indices  $\{i, \ell, m\}$ ;  $i > 0$  ( $i = 0$ ) stands for the  $i$ th discretized-continuum (ground) state and  $\ell$  and  $m$  are respectively the orbital angular momentum between the constituents (C and v) of the projectile and its projection

on the  $z$ -axis taken to be parallel to the incident beam. Note that we neglect the internal spins of C and v for simplicity. The impact parameter  $b$  is relegated to a superscript since it is not a dynamical variable. The total energy and the asymptotic wave number of P are denoted by  $E_c$  and  $K_c$ , respectively, and  $\mathcal{R}_{cc'}^{(b)}(z) = (K_{c'}R - K_{c'}z)^{i\eta_{c'}} / (K_cR - K_cz)^{i\eta_c}$  with  $\eta_c$  the Sommerfeld parameter. The local wave number  $K_c^{(b)}(z)$  of P is defined by energy conservation as

$$E_c = \sqrt{(m_P c^2)^2 + \left\{ \hbar c K_c^{(b)}(z) \right\}^2} + \frac{Z_P Z_T e^2}{R}, \quad (4)$$

where  $m_P$  is the mass of P and  $Z_P e$  ( $Z_T e$ ) is the charge of P (T). The reduced coupling-potential  $\mathfrak{F}_{cc'}^{(b)}(z)$  is given by

$$\mathfrak{F}_{cc'}^{(b)}(z) = \mathcal{F}_{cc'}^{(b)}(z) - \frac{Z_P Z_T e^2}{R} \delta_{cc'}, \quad (5)$$

where

$$\mathcal{F}_{cc'}^{(b)}(z) = \langle \Phi_c | U_{CT} + U_{vT} | \Phi_{c'} \rangle_\xi e^{-i(m'-m)\phi_R}. \quad (6)$$

The  $\Phi$  denotes the internal wavefunctions of P,  $\phi_R$  is the azimuthal angle of  $\mathbf{b}$  and  $U_{CT}$  ( $U_{vT}$ ) is the potential between C (v) and T consisting of nuclear and Coulomb parts. In actual calculations we use the multipole expansion  $\mathcal{F}_{cc'}^{(b)}(z) = \sum_\lambda \mathcal{F}_{cc'}^{\lambda(b)}(z)$ , the explicit form of which is shown in Ref. 3).

In order to include the dynamical relativistic effects described above, we make the replacement

$$\mathcal{F}_{cc'}^{\lambda(b)}(z) \rightarrow \gamma f_{\lambda, m-m'} \mathcal{F}_{cc'}^{\lambda(b)}(\gamma z). \quad (7)$$

The factor  $f_{\lambda, \mu}$  is set to unity for nuclear couplings, while for Coulomb couplings we take

$$f_{\lambda, \mu} = \begin{cases} 1/\gamma & (\lambda = 1, \mu = 0) \\ (\gamma^2 + 1)/(2\gamma) & (\lambda = 2, \mu = \pm 1) \\ 1 & (\text{otherwise}) \end{cases} \quad (8)$$

following Eqs. (1) and (2). Correspondingly, we use

$$\frac{Z_P Z_T e^2}{R} \delta_{cc'} \rightarrow \gamma \frac{Z_P Z_T e^2}{\sqrt{b^2 + (\gamma z)^2}} \delta_{cc'} \quad (9)$$

in Eqs. (4) and (5). The Lorentz contraction factor  $\gamma$  may have channel-dependence, i.e.,  $\gamma = E_c/(m_P c^2)$ , which we approximate by the value in the incident channel, i.e.,  $E_0/(m_P c^2)$ .

It should be remarked that we neglect the recoil motion of T in Eq. (3); this can be justified because we consider reactions in which T is significantly heavier than P and we only treat forward-angle scattering in the present study,<sup>5)</sup> as shown below. Note also that in the high incident-energy limit  $\mathcal{R}_{cc'}^{(b)}(z) \rightarrow 1$  and  $K_c^{(b)}(z) \rightarrow K_c$ , unless the energy transfer is extremely large. Thus, in this limit Eq. (3) becomes Lorentz covariant, as desired.

Using Eqs. (3)–(9), we calculate the dissociation observables in reactions of loosely bound nuclei  $^8\text{B}$  and  $^{11}\text{Be}$  on  $^{208}\text{Pb}$  targets. The internal Hamiltonian of P and the number of the states included are the same as in Ref. 12) except that we neglect the spin of the proton as mentioned above and thus change the depth of the  $p$ - $^7\text{Be}$  potential to reproduce the proton separation energy of 137 keV. The optical potentials between the constituents of P and T are the same as in Table I of Ref. 12). Note that the results shown below do not depend on the choice of these potentials significantly. The maximum value of the internal coordinate  $\xi$  is taken to be 200 fm. The maximum impact parameter is set to be 500 fm and 450 fm for, respectively,  $^8\text{B}$  and  $^{11}\text{Be}$  breakup reactions at 100 MeV/nucleon, while it is set to 400 fm for both reactions at 250 MeV/nucleon.

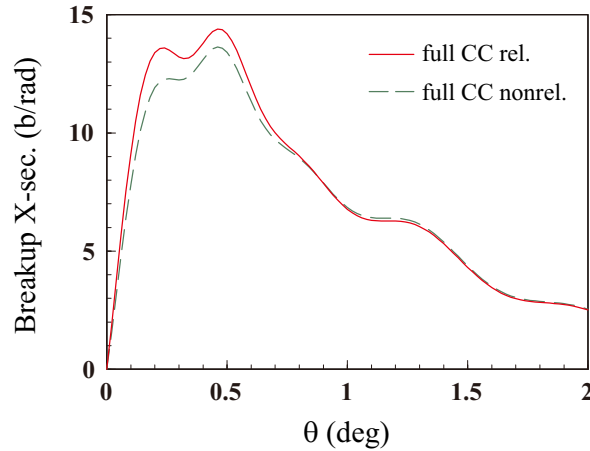


Fig. 1. The total breakup cross section for  $^8\text{B}+^{208}\text{Pb}$  at 250 MeV/nucleon, as a function of the scattering angle of the c.m. of the projectile after breakup. The solid and dashed lines show the results of the full CC calculation with and without the dynamical relativistic effects, respectively.

Figure 1 shows the total breakup cross section of  $^8\text{B}$  by  $^{208}\text{Pb}$  at 250 MeV/nucleon, as a function of the scattering angle  $\theta$  of the center-of-mass (c.m.) of the projectile after breakup. The solid and dashed lines represent the results of the E-CDCC calculation with and without the dynamical relativistic effects, respectively; in the latter we set  $\gamma = 1$  instead of the proper value 1.268 in Eqs. (7)–(9). Note that in all calculations shown in this work we use relativistic kinematics, so that our results probe only the relativistic effects on the dynamics. One sees that the dynamical relativistic correction gives significantly larger breakup cross sections for  $\theta \lesssim 0.7$  degrees; the difference between the two around the peak is sizable, i.e. of the order of 10–15 %.

Figure 2 shows the corresponding partial breakup cross sections as a function of  $b$ . One sees that for  $b \leq 50$  fm the difference between the two is negligibly small, while for  $b > 50$  fm a clear enhancement of the cross section due to dynamical relativistic effects is found. Since the nuclear coupling potentials in E-CDCC calculations for the reaction under study are limited to  $b$  less than about 15 fm, at the most, the enhancement of the breakup cross section shown in Fig. 1 is due to the dynamical

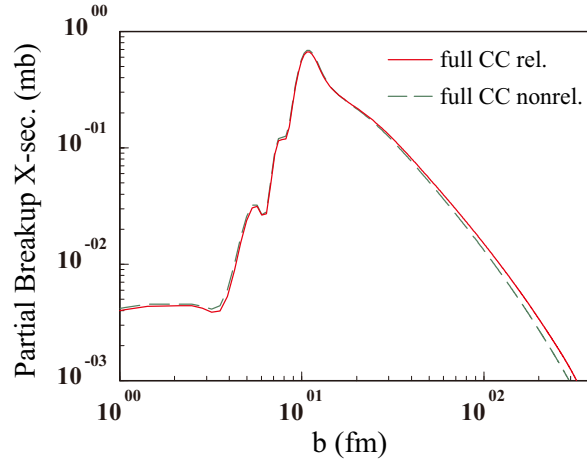


Fig. 2. Partial breakup cross sections as a function of  $b$  for  ${}^8\text{B}+{}^{208}\text{Pb}$  at 250 MeV/nucleon.

relativistic correction to the Coulomb potential. In other words, the effects of relativistic corrections in the nuclear potentials are negligible, which is a new important finding in the present study. This can be seen more clearly in Fig. 3, for the breakup cross sections calculated with the E-CDCC method, with only the nuclear coupling potentials. The relativistic and non-relativistic results in Fig. 3 agree very well with each other.

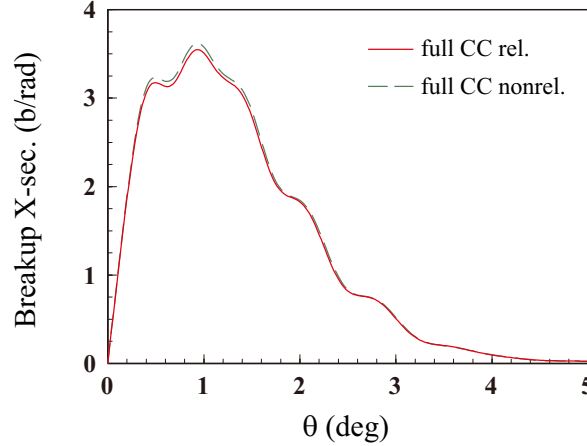


Fig. 3. Same as in Fig. 1 but only the nuclear coupling potentials are included in the E-CDCC calculation.

Next we investigate how the coupled-channel calculations affect the breakup cross section and the role of dynamical relativistic corrections. For this purpose, a first-order perturbative calculation is performed. This first-order calculation is consistent with the equivalent photon method, as described in Ref. 13). In fact, first-order Coulomb excitation can be expressed as  $d\sigma/dE_\gamma = N_{E\lambda}(E_\gamma)\sigma_\gamma^{(E\lambda)}(E_\gamma)$ , where  $N_{E\lambda}(E_\gamma)$  is the equivalent photon spectrum for the  $E\lambda$  multipolarity, and  $\sigma_\gamma^{(E\lambda)}(E_\gamma)$

is the corresponding photonuclear dissociation cross section. Using the expressions for  $N(E\lambda)$ ,  $\lambda = 1, 2$ , given in Ref. 13) with the matrix elements for the  $E\lambda$  operator used in the present work, we confirm that first order perturbation theory and the equivalent photon method yield exactly the same results, as expected.

We show in Fig. 4 the results of full-CDCC and the first-order calculation; the left (right) panel corresponds to the calculation with both nuclear and Coulomb breakup (only Coulomb breakup). In each panel the solid (dotted) and dashed (dash-dotted) lines show the results of the full CC (first-order perturbative) calculation with and without the relativistic correction, respectively.

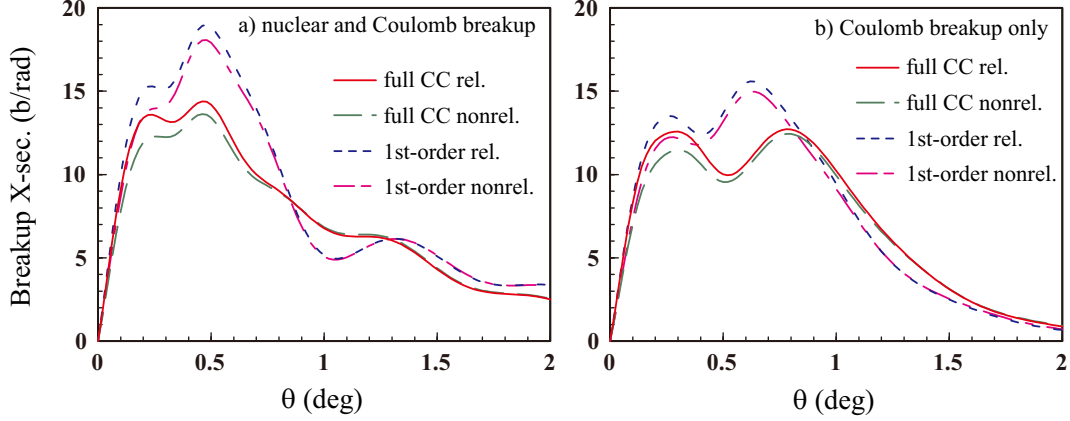


Fig. 4. The total breakup cross sections for  ${}^8\text{B}+{}^{208}\text{Pb}$  at 250 MeV/nucleon with nuclear and Coulomb breakup (left panel) and only Coulomb breakup (right panel). The solid (dotted) and dashed (dash-dotted) lines show the results of the full CC (first-order perturbative) calculation with and without the relativistic correction, respectively.

lines show the results of the full CC (first-order perturbative) calculation with and without the dynamical relativistic correction, respectively. One sees that relativistic corrections modify the first-order results in the same way as they do with the full CC calculation. We stress here, however, that since continuum-continuum couplings

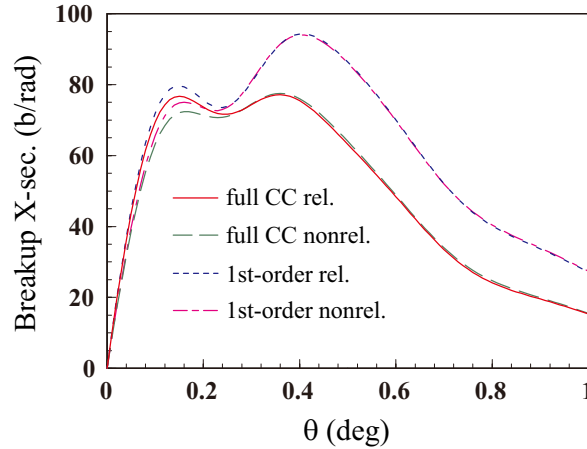


Fig. 5. Same as in Fig. 4a but for  ${}^{11}\text{Be}+{}^{208}\text{Pb}$  at 250 MeV/nucleon.

make relativistic effects non-linear (and non-trivial to interpret), one cannot infer the effect of relativistic corrections by simply carrying out first-order calculations. More seriously, the full CC and first-order calculations give quite different breakup cross sections even at forward angles. Full CC calculation is necessary to obtain a reliable breakup cross section to be compared with experimental data. In other words, continuum-continuum couplings are important in describing breakup processes even at intermediate energies. It is found that continuum-continuum couplings for both nuclear and Coulomb parts play significant roles.

In Fig. 5 we show the results for  $^{11}\text{Be}$  breakup by  $^{208}\text{Pb}$  at 250 MeV/nucleon, with  $\gamma = 1.268$ . Differences between the relativistic and nonrelativistic calculations appear below about 0.3 degrees for both full CC and first-order perturbative results, and the increase of the cross section around the peak is, as for the  $^8\text{B}$  breakup, about 10–15 %.

Figures 6 and 7 show, respectively, the results for  $^8\text{B}+^{208}\text{Pb}$  and  $^{11}\text{Be}+^{208}\text{Pb}$  at 100 MeV/nucleon. The main features of the results are the same as at 250 MeV/nucleon, except that the effects of relativity are somewhat reduced, i.e., the enhancement of the cross section at the peak is below the 10% level. This rather

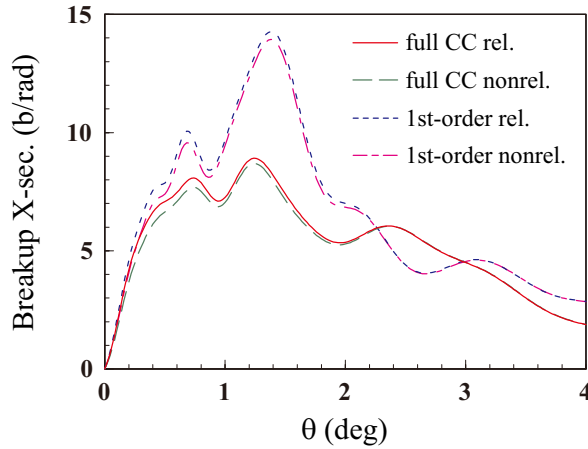


Fig. 6. Same as in Fig. 4a but for  $^8\text{B}+^{208}\text{Pb}$  at 100 MeV/nucleon.

small difference can still be important for some quantitative analysis, e.g. determination of the astrophysical factor  $S_{17}$  for the  $^7\text{Be}(p, \gamma)^8\text{B}$  reaction through  $^8\text{B}$  breakup reaction. In order to draw a definite conclusion, however, we need to quantitatively examine the approximations used to derive Eqs. (1) and (2), i.e., use of point charge for C, v and T, and also the far-field approximation.<sup>10)</sup> Moreover, an evaluation of quantum mechanical corrections to the breakup cross sections, which can be done by constructing hybrid scattering amplitudes,<sup>2),3)</sup> will be necessary. Nevertheless, relativistic effects on the breakup cross sections of about 15% found at 250 MeV/nucleon needs to be seriously addressed in the future.

In conclusion, we have evaluated the effects of relativistic corrections of the nuclear and Coulomb coupling potentials on the breakup cross sections of the weakly bound projectiles  $^8\text{B}$  and  $^{11}\text{Be}$  by  $^{208}\text{Pb}$  targets at 250 and 100 MeV/nucleon. The

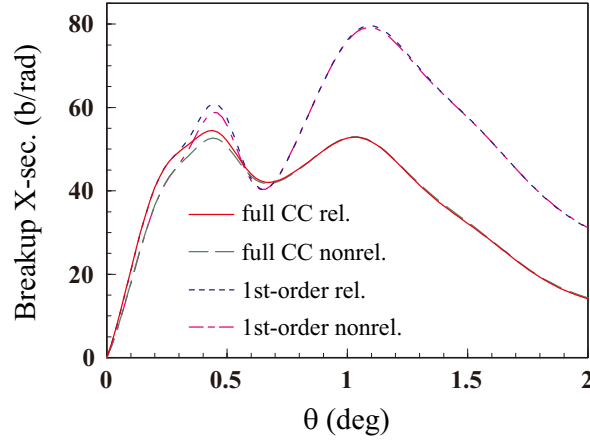


Fig. 7. Same as in Fig. 4a but for  $^{11}\text{Be}+^{208}\text{Pb}$  at 100 MeV/nucleon.

relativistic corrections modify appreciably the breakup cross sections, at the level of 15% (10%), in collisions at 250 (100) MeV/nucleon. This change is found to be due mainly to the modification of the Coulomb potential. We have shown that continuum-continuum couplings are also influenced by relativistic corrections and modify breakup cross sections appreciably. These important features have been widely ignored in the literature and deserve further theoretical studies. We have found quite strong relativistic effects on breakup energy spectra of  $^8\text{B}$ . More detailed and systematic analysis including this subject will be presented in a forthcoming paper.

This work was partially supported by the U.S. DOE grants DE-FG02-08ER41533 and DE-FC02-07ER41457 (UNEDF, SciDAC-2), and the JUSTIPEN/DOE grant DEFG02-06ER41407. The computation was carried out using the computer facilities at Research Institute for Information Technology, Kyushu University.

- 
- 1) I. Tanihata, Prog. Part. Nucl. Phys. **35**, 505 (1995) and references cited therein.
  - 2) K. Ogata, M. Yahiro, Y. Iseri, T. Matsumoto and M. Kamimura, Phys. Rev. C **68**, 064609 (2003).
  - 3) K. Ogata, S. Hashimoto, Y. Iseri, M. Kamimura and M. Yahiro, Phys. Rev. C **73**, 024605 (2006).
  - 4) M. Kamimura *et al.*, Prog. Theor. Phys. Suppl. **89**, 1 (1986); N. Austern *et al.*, Phys. Rep. **154**, 125 (1987).
  - 5) C. A. Bertulani, Phys. Rev. Lett. **94**, 072701 (2005).
  - 6) C. A. Bertulani, A. E. Stuchbery, T. J. Mertzimekis and A. D. Davies, Phys. Rev. C **68**, 044609 (2003).
  - 7) C. A. Bertulani, G. Cardella, M. De Napoli, G. Raciti, E. Rapisarda, Phys. Lett. **B650**, 233 (2007).
  - 8) H. Scheit, A. Gade, Th. Glasmacher, T. Motobayashi, Phys. Lett. **B659**, 515 (2007).
  - 9) H. Esbensen, Phys. Rev. **C78**, 024608 (2008).
  - 10) H. Esbensen and C.A. Bertulani, Phys. Rev. C **65**, 024605 (2002).
  - 11) H. Feshbach and M. Zabeck, Ann. of Phys. **107** (1977) 110.
  - 12) M. S. Hussein, R. Lichtenthäler, F. M. Nunes and I. J. Thompson, Phys. Lett. **B640**, 91 (2006).



- 13) C. A. Bertulani and G. Baur, Phys. Rep. **163**, 299 (1988).